

Seismic Fragility Assessment of a Multi-span Continuous Highway Bridge Isolated by Shape Memory Alloy Restrainer and Lead Rubber Bearing



A. Rahman Bhuiyan

*Department of Civil Engineering, Chittagong University of Engineering and Technology,
Chittagong-4349, Bangladesh*

M. Shahria Alam

School of Engineering, University of British Columbia, Kelowna, BC, V1V1V7, Canada

SUMMARY:

Seismic vulnerability assessment of a three-span continuous highway bridge, restrained by Ni-Ti based shape memory alloy (SMA) and isolated by means of lead rubber bearing (LRB), has been carried out. The analytical simulation method based on nonlinear incremental dynamic analysis results is used in evaluating the seismic fragility functions to describe the seismic vulnerability of the bridge components (piers and lead rubber bearings). A 2-D finite element model scheme, with nonlinear force-displacement relationships for the bridge piers, LRBs, and SMA restrainers, is used in modeling the bridge. A total of 20 moderate earthquake records are used in the analysis. The seismic fragility functions of the bridge components are generated, which are then combined to approximate the overall system fragility functions at different damage states. The study shows that the bridge piers with SMA restrainers lead to relatively higher seismic vulnerability than that without SMA restrainers. The LRBs with SMA restrainers have revealed comparatively less seismic vulnerability than without SMA restrainers.

Keywords: Seismic fragility, lead rubber bearing, shape memory alloy, incremental dynamic analysis

1. INTRODUCTION

Highway bridges are the most common and critical civil infrastructure components of a transportation network as they play important roles in evacuation and emergency routes for rescues, first-aid, firefighting, medical services and transporting disaster commodities. In order to improve the seismic performance and subsequently reduce the seismic vulnerability of both new and retrofitted bridges, different forms of seismic isolation devices have been widely used for the last few decades (Kelly, 1997; Skinner et al., 1993). Field evidence on the seismic response of isolated bridges during recent earthquakes (Chaudhury et al., 2001), analytical studies and experimental research (Dall'Asta and Ragni, 2006; Hwang et al., 2002) have shown that isolation devices can suppress the transmission of the input earthquake energy, which helps improve the seismic performance and subsequently reduce the cost for repair and rehabilitation after earthquakes.

Laminated rubber bearings and sliding bearings are the two major types of seismic isolation devices, which are usually adopted for seismic protection of highway bridges. Due to the capability of supporting large loads while sustaining large movements with little or no maintenance requirement (Ali and Ghaffar, 1995), the laminated rubber bearings have been applied more frequently in highway bridges in recent years. Three types of laminated rubber bearings are widely used for this purpose: natural rubber bearing (NRB), lead rubber bearing (LRB), and high damping rubber bearing (HDRB). LRBs possess various mechanical properties, which are influenced by their compounding effect (Hwang et al., 2002), nonlinear elasto-plastic behavior (Bhuiyan, 2009) and low strain-rate dependent viscosity property (Bhuiyan, 2009).

Laminated rubber bearings initiate some inherited problems, such as (i) instability due to large deformation, and (ii) un-recovered residual deformation, and (iii) the necessity for replacement of the deformed bearings after a strong earthquake. In order to overcome fully/partially the above mentioned limitations of the rubber bearings, shape memory alloys (SMA) accompanied with laminated rubber bearings are reported to employ in the seismic isolation of highway bridge (DesRoches and Delemont, 2002; Ozbulut and Hurlebaus, 2011). The super-elasticity and hysteresis property of the SMA allows it to incorporate with laminated rubber bearings to reduce the residual deformation of the bridge system. The application of SMA, due to its inherited restoring and energy dissipation capacity, is getting wide acceptance in seismic protection of highway bridges (Ozbulut and Hurlebaus, 2011 and the references cited therein).

The vulnerability assessment of bridges is widely recognized to be useful for prioritization of seismic retrofitting decisions, disaster response planning, estimation of direct monetary loss, and evaluation of loss of functionality of highway systems in the event of an earthquake. The seismic vulnerability of highway bridges is usually expressed in the form of fragility curves, which display the conditional probability where the structural demand (structural response) caused by various levels of ground shaking exceeds the structural capacity defined by a damage state. There are different fragility-curve generation methodologies involving probabilistic seismic performance evaluation of highway bridges (Karim and Yamazaki, 2007). Though all methodologies have their own limitations in evaluating the probabilistic seismic performance of highway bridges, fragility assessment methodologies using analytical approaches have widely adopted since they are more readily applicable to bridge types and geographical regions where seismic bridge damage records are insufficient.

The objective of this work is to carry out the seismic vulnerability assessment of a three-span continuous highway bridge isolated by LRBs and SMA restrainers. In this regard, analytical based simulation method is used to evaluate the seismic fragility of the bridge based on the results obtained from nonlinear incremental dynamic analysis (IDA). A 2-D finite element model scheme with nonlinear force-displacement relationships for the bridge piers and the isolation bearings are used in analytical modeling of the bridge. Nonlinear incremental dynamic analyses of the isolated bridge are then performed for a total of 20 earthquake excitations with peak ground accelerations (PGA) ranging from 0.45g to 1.07g. Each record is first scaled at selective earthquake intensities up to 2.0 g and then incremental dynamic analysis is carried out at each level of intensity. The seismic responses of the bridge components (pier and isolation bearing) are utilized to evaluate the likelihood of exceeding the seismic capacity of each component.

2. MODELING OF BRIDGE

2.1. Physical Model

A three-span continuous highway bridge isolated by laminated rubber bearings and SMA restrainers is used in the current study. The bridge consists of continuous reinforced concrete (RC) deck-steel girder isolated by laminated rubber bearings installed below the steel girder supported on RC piers. In addition, two SMA bars are used at each bridge pier being attached between top of bridge pier and bottom of the girder. The superstructure consists of 260 mm RC slab covered by 80 mm of asphalt layer. The height of the continuous steel girder is 1800 mm. The substructures consist of RC piers and footings supported on shallow foundation. The reinforcement details of the bridge pier consist of D29 (diameter 29 mm) longitudinal reinforcements along the longer direction being distributed @ 200 mm c/c except at the corners where the spacing of the reinforcements is 125 mm c/c and D29 (diameter 29 mm) reinforcements along the shorter direction being distributed @ 200 mm c/c except at the corners where spacing is limited to 150 mm c/c. The hoop reinforcements in both directions are D22 (diameter 22 mm) being distributed @ 125 mm c/c. The geometry and material properties of laminated rubber bearings and shape memory alloy are presented in Table 1.

Table 1. Geometries and materials properties of the isolation bearings and Ni-Ti SMA

Properties	Values
Cross-section of the bearing (mm^2)	600
Thickness of rubber layers (mm)	75
Number of rubber layers	6
Thickness of steel layer (mm)	3.0
Nominal shear Modulus (MPa)	1.2
Number of lead plugs	4
Diameter of lead plugs (mm)	90
Cross-section of SMA restrainer bar (mm^2)	1256
Length of SMA restrainer bar (mm)	2500

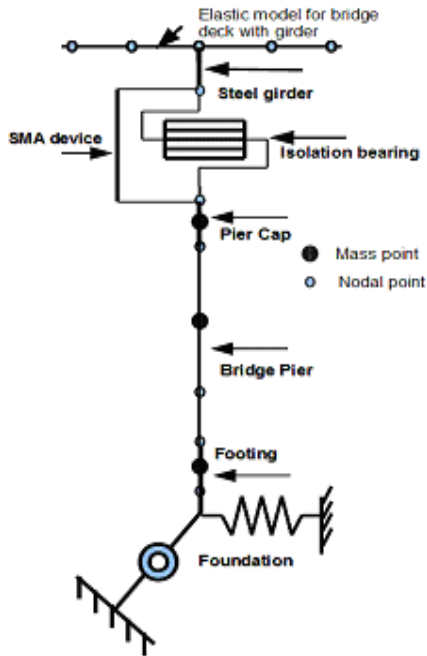


Figure 1. 2-D finite element model of a typical bridge pier

2.2. Analytical Model

The entire system is approximated as a continuous 2-D finite element frame using the SeismoStruct nonlinear analysis program (SeismoStruct, 2011). Analytical model of a typical bridge pier with girder is shown in Figure 1. A finite element model with frame and spring elements is used to approximate the continuous system with a finite number of degrees of freedom. The superstructure and substructure of the bridge are modeled as a lumped mass system divided into a number of small discrete segments. The mass of each segment is assumed to be distributed between the two adjacent nodes in the form of point mass. The details of modeling of a typical bridge pier along with deck are presented in Figure 1. The superstructure consisting of RC bridge deck and steel girders is modeled using linear beam-column elements so that the superstructure remains elastic under the seismic loads applied in the longitudinal direction. It should be noted that the stiffness of the superstructure does not have a

significant effect on the seismic response of the bridge (Ghabarah and Ali, 1988) since the longitudinal response is typically governed by the isolation bearings, bridge piers, and foundation (Choi et al., 2004). The bridge piers are modeled using the fiber elements. Each fiber has a stress-strain relationship, which can be specified to represent unconfined concrete, confined concrete, and longitudinal steel reinforcement. The confinement effect of the concrete section is considered on the basis of reinforcement detailing as discussed in the preceding section. The distribution of inelastic deformation and forces is sampled by specifying cross-section slices along the length of the element. The pier footings are modeled using linear elastic elements. The footing-foundation movement is modeled using two linear translation and rotation springs.

The mechanical behavior of laminated rubber bearings can be characterized by three distinct features: a high initial stiffness at very small strain levels, an almost constant stiffness at small to medium strain levels followed by a high stiffness due to its inherently occupied strain hardening features. So, a constitutive model with the ability to replicate the strain-rate and the strain level dependent mechanical behavior of laminated rubber bearing is required for simulating the mechanical responses when subjected to earthquake induced ground motions. However, for brevity, the current study considers the design bilinear model (Figure 2) as proposed in different code specifications (AASHTO, 2000; JRA, 2002). The model parameters of the bearings are estimated as per recommendations of JRA (2002) and presented in Table 2.

In general, the constitutive model of SMA is very complicated in a sense that it depends upon many factors, such as strain rates (Auricchio et al., 1997), strain magnitude and strain history (Wei et al., 2002). Three categories of constitutive models are used for characterizing the superelasticity and damping properties of SMA, such as parametric, nonparametric and differential equation-based models. However, the differential equation-based constitutive model (Auricchio et al., 1997; Wei et al., 2002) is widely used for SMA since it is capable of using in continuum mechanics based FE algorithms considering small and finite deformations and subsequently in finite element based professional software packages, such as ANSYS (2010) and SeismoStruct (2011), etc. Table 3 shows the parameters of Ni-Ti based SMA (Figure 4) used in the analysis of this study.

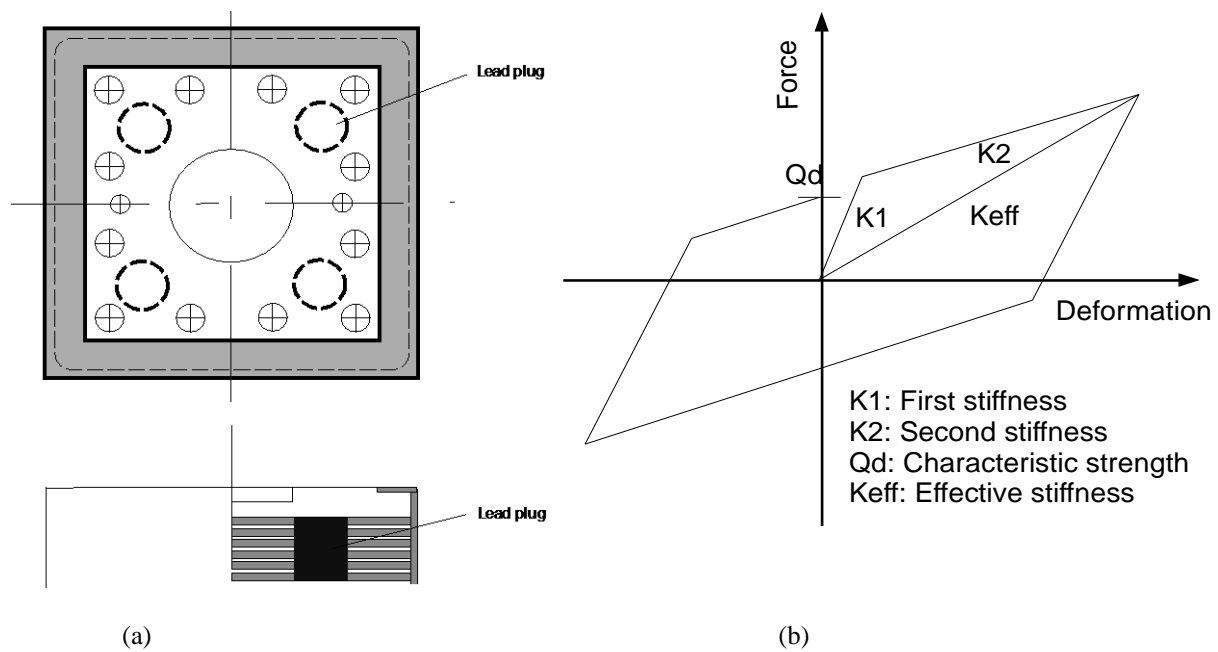


Figure 2. (a) Arrangement of LRB, and (b) bilinear model of LRB used in AASHTO (2000) and JRA (2002).

Table 2. Design parameters of the bearing

Parameters	LRB
Elastic stiffness, K1(kN/m)	30000
Post yield stiffness, K2, (kN/m)	4221
Characteristic strength, Qd (kN)	200
Effective stiffness, Keff (kN/m)	5840
Effective damping ratio (%)	16.7

Table 3. Constitutive parameters of Ni-Ti based SMA

Parameters	Unit	Value
Austenite to martensite starting stress, f_y	MPa	410
Austenite to martensite finishing stress, f_{P1}	MPa	470
Martensite to austenite starting stress, f_{T1}	MPa	170
Martensite to austenite finishing stress, f_{T2}	MPa	140
Yield strain limit, ε_y	%	1
Recoverable pseudoelastic strain limit, ε_{Pl}	%	7

3. SEISMIC FRAGILITY FUNCTION

Probabilistic Seismic Demand Model (PSDM) is employed to derive the analytical fragility curves using nonlinear time-history analyses of the bridge system. The PSDM establishes a correlation between the engineering demand parameters (EDP) and the ground intensity measures (IM). In the current study, the ductility of bridge pier and horizontal deformation of isolation bearing are considered as the two EDPs, and the peak ground acceleration (PGA) is utilized as intensity measure (IM) of each ground motion record. Only the Incremental Dynamic Analysis (IDA) method is utilized in evaluating the seismic fragility functions of the bridge components and system. The IDA method requires more computational efforts in scaling of earthquake ground motion records to be applied in nonlinear time history analysis at each IM level. Every ground motion record is scaled up to a maximum PGA of 2.0g. The occurrence ratio at a specified damage state (DS) is computed and directly used as the damage probability at the given IM level, i.e. the damage probability is calculated as the ratio of the number of damage cases n_i for the damage state i over the number of total simulation cases N :

$$P[EDP > DS_i | IM] = \frac{n_i}{N} \quad (1)$$

The fragility curves as derived using IDA approach can be expressed in most cases using a lognormal cumulative distribution function:

$$P[EDP > DS_i | IM] = \int_{-\infty}^{IM} \frac{1}{IM\sqrt{2\pi\xi_{IM}^2}} \exp\left[-\frac{[\ln(IM) - \lambda]^2}{2\xi_{IM}^2}\right] d(IM), \quad (2)$$

where λ and ξ^2 denote mean and standard deviation of IMs based of lognormal distribution, respectively.

4. CHARACTERIZATIONS OF DAMAGE STATES

For seismically isolated highway bridges with continuous composite deck-girder system, bridge piers and isolation bearings are the most critical components, which are often forced to enter into nonlinear range of deformations under strong earthquakes. Different forms of EDPs, ductility for bridge piers, residual deformation of bridge pier and horizontal deformation for isolation bearings, are used to measure the damage state (DS) of the bridge components. A capacity model is needed to measure the damage of bridge component based on prescriptive and descriptive damage states in terms of EDPs (FEMA, 2003, Choi et al., 2004). Four damage states as defined by HAZUS (FEMA, 2003) are

commonly adopted in the seismic vulnerability assessment of engineering structures, namely slight, moderate, extensive and collapse damages. Table 4 summarizes the definitions of various damage states and their corresponding damage criteria available in literature. The damage states of isolation devices are determined based on experimental observation as well as the consideration of resulting pounding and unseating. Either the bearing displacement or shear strain is used to describe the damage states as shown in Table 4.

Previous studies (Bhuiyan, 2009) show that the mechanical behavior of laminated rubber bearings portrays three distinct features such as initial high stiffness at very low strain levels, almost constant stiffness at low to moderate strain levels due to its Payne's effect and finally high stiffness at high strain levels (e.g. 150%) due to its strain hardening effects. Moreover, strain-rate and temperature induced viscosity property is depicted in the bearings, especially in high damping rubber bearings (Bhuiyan et al., 2009, Bhuiyan, 2009). Although the modern isolation bearings can experience shear strain up to 400% before failure, such large shear strain will result in large displacement and can cause significant pounding or unseating problem in the bridge system. Therefore, once the shear strain exceeds 250%, it is considered as complete damage of the bearing (JRA, 2002). In this study, the shear strain for isolation bearings and the displacement ductility for the bridge pier are adopted as damage index to capture the damage states.

Table 4. Damage/limit state of bridge components

Damage State →		Slight (DS=1)	Moderate (DS=2)	Extensive (DS=3)	Collapse (DS=4)	Reference
Bridge components	Physical phenomenon	Cracking and spalling	Moderate cracking and spalling	Degradation without collapse	Failure leading to collapse	FEMA, 2003
Bridge pier	Section ductility μ_k	$\mu_k > 1$	$\mu_k > 2$	$\mu_k > 4$	$\mu_k > 7$	Choi et al. 2004
	Displacement ductility μ_d	$\mu_d > 1.0$	$\mu_d > 1.2$	$\mu_d > 1.76$	$\mu_d > 4.76$	Hwang et al. 2001
	Residual displacement, δ_r (mm)	$\delta_r > 0.0$	$\delta_r > 12$	$\delta_r > 47$	$\delta_r > 233$	
Isolation bearing	Displacement δ (mm)	$\delta > 0$	$\delta > 50$	$\delta > 100$	$\delta > 150$	Choi et al. 2004
	Shear strain γ (%)	$\gamma > 100$	$\gamma > 150$	$\gamma > 200$	$\gamma > 250$	Zhang and Huo 2009

5. SEISMIC GROUND MOTION RECORDS

A suite of 20 earthquake ground motion records, which are assigned as medium to strong magnitude earthquake ground motions (JRA, 2002), with PGA values ranging from 0.45g to 1.07g have been considered in the current study. Figure 4 shows the acceleration response spectra with 5 percent damping ratio of the recorded ground motions. The mean amplitude of the earthquake records is shown by solid thick line in the figure.

6. NUMERICAL RESULTS AND DISCUSSION

In order to assess the seismic vulnerability of a three-span continuous highway bridge, seismic fragility curves for the piers and isolation bearings are generated using the numerical results obtained from the nonlinear incremental dynamic analysis. The bridge is isolated with two types of laminated rubber bearings along with shape memory alloy restrainers. Assuming a lognormal distribution with respect to the median of seismic intensity (PGA), the fragility curves for two bridge components, pier and isolation bearing, are generated using Eqs.(1) and (2) and calibrated with the capacity limit states as shown in Table 1. In this regard, a number of incremental dynamic analyses of the bridge, subjected to longitudinal excitations using 20 ground motion records of PGA magnitudes ranging from 0.45 to 1.07g, are carried out. Each ground motion record is scaled at different intensity levels up to 2.0g PGA, which is then used in the incremental dynamic analysis. Nonlinear models for bridge piers, isolation bearings and shape memory alloys are considered in the present analysis. Moreover, the Raleigh damping approach is employed in order to estimate the damping of the bridge.

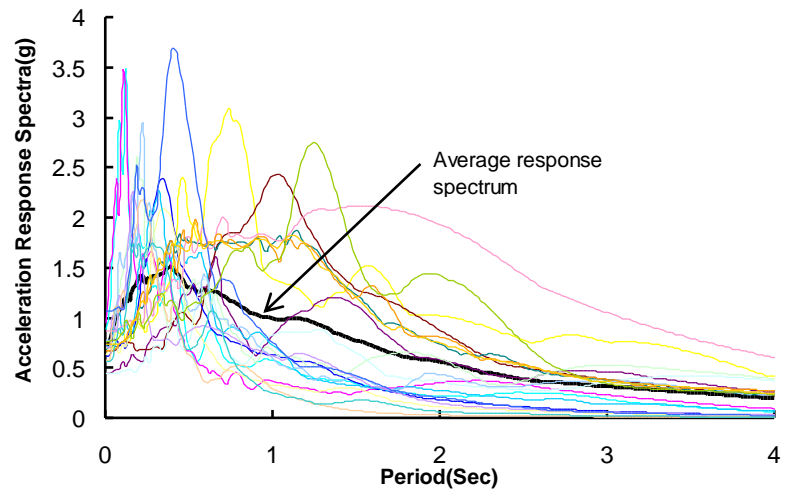


Figure 3. Response acceleration spectra of a suite of 20 near-fault earthquake ground motion records. The peak ground accelerations range from 0.45g to 1.07g.

Figures 4 to 6 present the fragility curves of the bridge at component levels, i.e. bridge piers and isolation bearings. Figures 4 (a) and (b) present the fragility curves for the bridge pier isolated by LRB without and with SMA restrainers, respectively. The most vulnerable pier is considered in deriving the fragility curves for different damage states (DS) as recommended by HAZUS-MH (FEMA, 2003), such as *slight, medium, extensive and collapse*. As can be observed from Figs. 4(a) and (b), the inclusion of SMA device in the isolation system significantly increases the seismic vulnerability of the bridge pier in all damage states at each earthquake intensity level. This can be attributed that the

inclusion of SMA device induces an additional stiffness to the bridge system causing a higher seismic force demand being attracted to the bridge pier (Wilde et al., 2000).

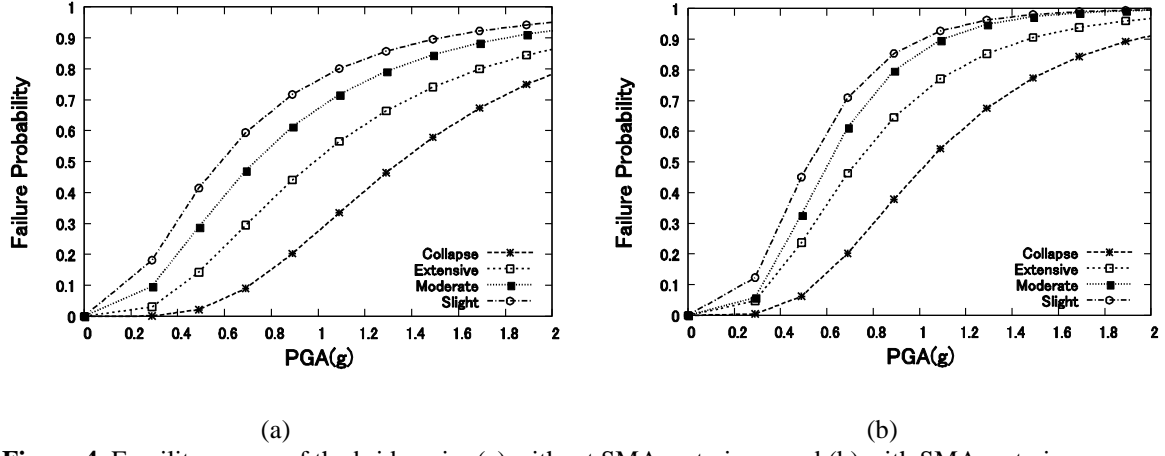


Figure 4. Fragility curves of the bridge pier (a) without SMA restrainers and (b) with SMA restrainers

Figures 5(a) and (b) illustrate the fragility curves in terms of residual displacements of the bridge piers without and with SMA restrainers, respectively. From each figure it can be observed that the inclusion of SMA restrainer in the isolation system causes a little increase in the seismic fragility of the bridge pier for a given damage state.

Figures 6 (a) and (b) display the fragility curves for the LRB without and with SMA restrainers. A total of four isolation bearings are used in the bridge to accommodate the vertical and lateral deformations as experienced from the vertical compressive loadings of the bridge deck and the earthquake ground motions. Only the most vulnerable bearing is utilized to derive the fragility curves. From each figure it is revealed that the inclusion of SMA restrainer in the isolation system causes a little increase in the seismic fragility of the LRB for the given damage states, which further induces the seismic vulnerability of the bearing and the bridge deck.

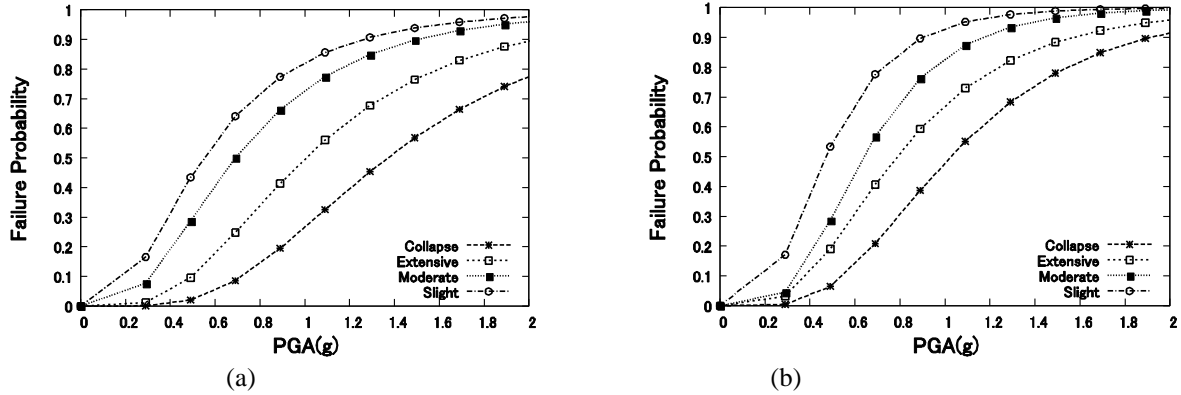


Figure 5. Fragility curves of the residual displacement of bridge pier isolated by lead rubber bearings (a) without SMA restrainers (b) with restrainers

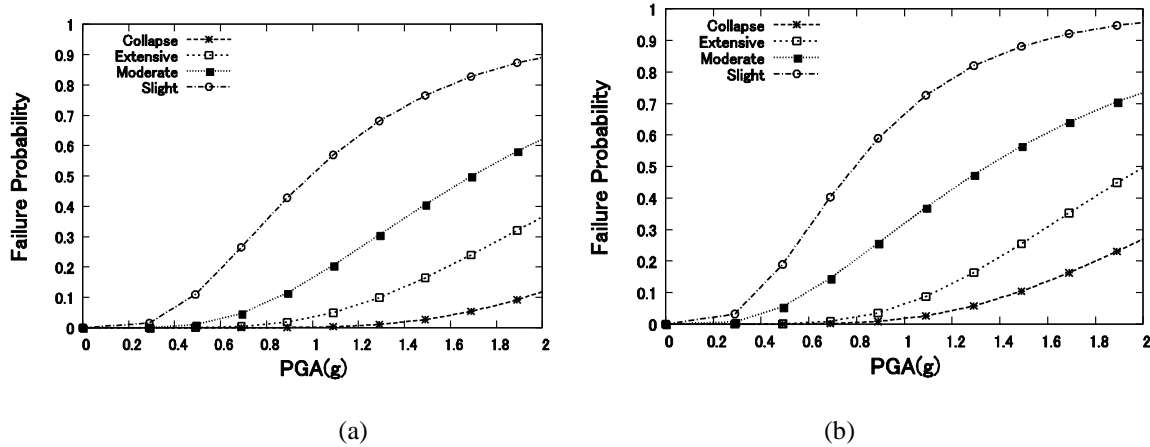


Figure 6. Fragility curves of lead rubber bearings (a) without SMA restrainers and (b) with SMA restrainers.

7. CONCLUDING REMARKS

This study utilizes analytical simulation method to conduct seismic fragility assessment of a three-span continuous highway bridge fitted with SMA restrainer and base isolation bearings. The fragility curves for bridge components (pier and isolation bearing) are generated based on the IDA-based scaling approach using 20 near-field earthquake ground motion records. The numerical results generally show that bridge piers are more susceptible to the given seismic ground motions as compared to the isolation bearings. Specifically, the seismic fragility of the bridge pier increases with the inclusion of the SMA restrainers in the isolation system. The fragility curves as obtained for the bridge system considered in this study can be used to estimate the potential losses incurred from earthquakes, retrofitting prioritization and post-earthquake rehabilitation decision making.

REFERENCES

- Ali, H.M., and Abdel-Ghaffar, A.M. (1995). Modeling of rubber and lead passive-control bearings for seismic analysis. *Journal ASCE Structural Engineering* **121**, 1134-1144.
- American Association of State Highways and Transportation Officials (AASHTO), (2000). *Guide specification for seismic isolation design*, 2nd edition, Washington D.C., USA
- ANSYS, Inc. , (2010). ANSYS version 12.0. ANSYS, Inc.
- Auricchio, F., Taylor, R.L. and Lubliner, J. (1997). Shape-memory alloys: macromodelling and numerical simulations of the superelastic behavior. *Computer Methods in Applied Mechanics and Engineering* **146**, 281-312.
- Bhuiyan, A.R., (2009). Rheology modeling of laminated rubber bearings for seismic analysis, PhD Dissertation, Graduate School of Science and Engineering, Saitama University, Japan.
- Bhuiyan, A.R., Okui, Y., Mitamura, H. and Imai, T., (2009). A rheology model of high damping rubber bearings for seismic analysis: identification of nonlinear viscosity. *International Journal of Solids and Structures* **46**, 1778-1792.
- Chaudhary, M.T.A., Abe, M., and Fujino, Y., (2001). Performance evaluation of base- isolated Yama-agé bridge with high damping rubber bearings using recorded seismic data. *Engineering Structures* **23**, 902-910.
- Choi, E., DesRoches, R. and Nielson, B.G., (2004). Seismic fragility of typical bridges in moderate seismic zones, *Engineering Structures* **26**, 187-199
- Dall'Asta, A., and Ragni, L., (2006). Experimental tests and analytical model of high damping rubber dissipating devices, *Engineering Structures* **28**, 1874-1884.
- DesRoches, R., Delemont, M. (2002). Seismic retrofit of simply supported bridges using shape memory alloys, *Engineering Structures* **24**, 325-332.
- Federal Emergency Management Agency (FEMA), (2003). HAZUS-MH software, Washington DC.
- Ghobarah, A. and Ali, H.M., (1988). Seismic performance of highway bridges. *Engineering Structures* **10**, 157-166.

- Hwang, H., Liu, J. B., Chiu, Y. H. (2001). Seismic fragility analysis of highway bridges. MAEC report: project MAEC RR-4. Urbana: Mid-America Earthquake Center
- Hwang, J.S., Wu, J. D., Pan, T. C., and Yang, G., (2002). A mathematical hysteretic model for elastomeric isolation bearings. *Earthquake Engineering and Structural Dynamics*. **31**:771-789.
- Japan Road Association, 2002. *Specifications for highway bridges*, Part V: Seismic design, Tokyo, Japan.
- Karim, K.R., and Yamazaki, F., (2007). Effect of isolation on fragility curves of highway bridges based on simplified approach. *Soil Dynamics and Earthquake Engineering* **27**, 414-426.
- Kelly, J.M., 1997, *Earthquake resistant design with rubber*, 2nd edition, Springer-Verlag Berlin Heidelberg, New York.
- Ozbulut, O.E., and Hurlebaus, S., (2011). Seismic assessment of bridge structures isolated by a shape memory alloy/rubber-based isolation system. *Smart Materials and Structures* **20**, 015003.
- SeismoStruct (2011). SeismoStruct help file. Available from www.seismsoft.com
- Skinner, R.I., Robinson, W.H., and McVerry, G.H., (1993). *An introduction to seismic isolation*, DSIR Physical Science, Wellington, New Zealand.
- Wei, Z., MA, H., Sun, D., (2002). A mathematical model for pseudoelasticity of shape memory alloy and its application in passive control. *Journal of Vibration and Control* **8**, 41-49.
- Wilde, K., Gardoni, P., and Fujino, Y., (2000). Base isolation system with shape memory alloy device for elevated highway bridges. *Engineering Structures* **22**, 222–229.
- Zhang, J. and Huo, Y., (2009). Evaluating effectiveness and optimum design of isolation devices for highway bridges using the fragility function method. *Engineering Structures* **31**, 1648-1660.